Electronic Supplementary Material (ESI) for Catalysis Science & Technology.

Supporting Information

Versatile catalysts constructed from hybrid polyoxomolybdates for simultaneously detoxifying sulfur mustard and organophosphate simulants

Yujiao Hou, Haiyan An,* Shenzhen Chang, Jie Zhang

College of Chemistry, Dalian University of Technology, Dalian 116023, P. R. China

CONTENTS:

---

*Corresponding author. Tel: +86-411-84657675. E-mail address: anhy@dlut.edu.cn

I. Supplementary experiments

Materials and methods

We used chemicals that were commercially purchased without further purification. Elemental analyses (H and N) were performed on a Perkin-Elmer 2400 CHN elemental analyzer; As, Te, Mo, Co, Ni, Mn, Zn, K, Na, Rb, and Cs were analyzed on a PLASMA-SPEC (I) ICP atomic emission spectrometer. **CAUTION:** The raw materials of the synthesis (As_2O_3 and Na_2TeO_3) are toxic and must be handled by trained personnel using applicable safety procedures in a closed system or in a hood under good ventilation. We detected the IR spectra using KBr pellets as the background in the range 400–4000 cm^{-1} on an Alpha Centaur FT/IR spectrophotometer. TG analyses were performed in flowing N_2 at a heating rate of 10°C min^{-1} on a Perkin-Elmer TGA7 instrument. The PXRD patterns of the samples were recorded on a Rigaku Dmax 2000 X-ray diffractometer with graphite monochromatized Cu-Ka radiation (λ = 0.154 nm) and 2θ varying from 5° to 50°. The diffuse reflectivity spectra were performed on finely ground samples with a Cary 500 spectrophotometer equipped with a 110 mm diameter integrating sphere, which were measured from 200 to 800 nm. The GC analysis was performed with an Agilent HP6890 spectrometer with a flame ionization detector, which was used to monitor the conversion and selectivity. GC−MS at the final time point was used to confirm the identity of the products. The GC−MS spectra were measured on an Agilent HP6890/5973MSD spectrometer. ^{1}HNMR spectroscopy was also used to monitor conversation and ascertain the product. And ^{1}HNMR spectra were collected on a 500 MHz Bruker Avance III system in $CDCl_3$.

Synthesis of $K_3[AsMo_6O_{21}(PABA)_3]\cdot nH_2O$ (13)

The compound was synthesized according to the literature: Na_2MoO_4 (0.145 g, 0.6 mmol), As_2O_3 (0.197 g, 0.1 mmol), and PABA (0.0411g, 0.3mmol) were dissolved in 20 mL of water. The pH value of the mixture was adjusted to 3.5 with HCl solution under stirring. The solution was stirring for one hour at room temperature. Then, the solution was heated and stirred for one hour at 80 °C. The filtrate was kept undisturbed for two weeks under ambient conditions. and then colorless crystals were isolated. FTIR data (cm^{-1}): 3442 (s), 3070 (m), 1564 (s), 1434 (s), 1441 (w), 1316 (w), 1111(m), 921(w), 889(s) 772 (w), 690 (m), 534 (m).

Synthesis of $K_6Na_2H_2[(H_2O)_6Co][AsMo_6O_{21}(Ala)_3]_4\cdot 41H_2O$ (14)

The synthetic procedure was similar to that used for **1**, with the organic ligand Ala (0.0267 g, 0.3 mmol) alone instead of PABA (0.0411g, 0.3mmol). The filtrate was kept undisturbed for two weeks under ambient conditions, and then pink crystals were isolated in about 32% yield (based on Mo). Calcd for **14**: Mo, 37.16 As, 4.84; Co, 0.95; Na, 0.74; K, 3.79; C, 6.98; N, 2.71; H, 2.83 (%). Found: Mo, 37.55; As, 5.11; Co, 1.05; Na, 0.80; K, 3.39; C, 7.21; N, 2.55; H, 2.76 (%). FTIR data (cm^{-1}): 3432 (s), 3139 (m), 1586 (s), 1435 (s), 1328 (w), 1294 (w), 1107(w), 914(m), 888(s), 772 (w), 668 (m), 505(w), 443 (m).

Synthesis of $K_{10}[(H_2O)_6Co][AsMo_6O_{21}(PHBA)_3]_2\cdot 23H_2O$ (15)

The synthetic procedur was similar to that used for **1**, with the organic ligand PHBA (0.0411 g, 0.3 mmol) alone instead of PABA (0.0411g, 0.3mmol). The filtrate was kept undisturbed for two weeks under ambient conditions, and then pink crystalswere

isolated in about 45% yield (based on Mo). Calcd for **15**: Mo, 30.56 As, 3.98; Co, 1.56; K, 10.38; C, 13.39; H, 2.35 (%). Found: Mo, 30.85; As, 4.11; Co, 1.45; K, 9.99; C, 13.21; H, 2.56 (%). FTIR data (cm^{-1}): 3377 (s), 3173 (m), 1598 (s), 1439 (s), 1410 (s), 1242 (m), 1170(m), 1104(w), 892(m), 786 (w), 675 (m), 503(w), 441 (w).

Catalytic oxidation of CEES

The evaluation of 2-chloroethyl ethyl sulfide (CEES) oxidation was performed as follows. Catalyst (2.5 μmol) was added acetonitrile (0.5 mL), followed by addition of CEES (0.25 mmol) and naphthalene (internal standard, 0.25mmol). After stirring the mixture at room temperature, H_2O_2 (0.28 mmol) was added dropwise. The reaction was monitored by gas chromatography at various time intervals. The catalytic reaction was carried out at room temperature for 12 minutes.

Catalytic hydrolysis of DECP

The hydrolysis reactions of diethyl cyanophosphonate (DECP) were performed as follows. Catalyst (0.6 μmol) was added to the mixture of H_2O (50 μL) and DMF (600 μL), followed by addition of DECP (1 mmol) and naphthalene (internal standard, 0.25mmol). The catalytic reaction was carried out at room temperature for 10 minutes. The reaction was monitored by gas chromatography at various time intervals. After the catalytic reactions was finished, the reusability of the hydrolysis reactions was continuously tested by adding the same amount of DECP (1 mmol) to the above reaction vessel under the similar situations.

Catalytic hydrolysis of DECP in the presence of H_2O_2

Catalyst (0.6 μmol) was added to the mixture of H_2O (50 μL) and DMF (600 μL),

followed by addition of DECP (1 mmol) H_2O_2 (0.5 mmol) and naphthalene (internal standard, 0.25mmol). The catalytic reaction was carried out at room temperature for 10 minutes. The reaction was monitored by gas chromatography at various time intervals.

Degradation of CEES and DECP at the same time

The oxidation of CEES and hydrolysis of DECP were performed in the same reaction vessel. Catalyst (2.5 μmol) was added DMF (600 μL) and H_2O (50 μL), followed by addition of CEES (0.25 mmol), DECP (1 mmol), H_2O_2 (0.28 mmol), and naphthalene (internal standard, 0.25mmol). The catalytic reaction was carried out at room temperature for 12 minutes. The reaction was monitored by gas chromatography at various time intervals.

Warning: HCN (one product of hydrolysis of DECP) is dangerous. The experiment must be done in a closed system or in a hood under good ventilation and using the safeguard procedures.

X-ray crystallography.

A Bruker Smart CCD diffractometer with Mo Kα radiation (λ = 0.71073 Å) was used to collect the crystallographic data of four compounds at 293 K or 220 K by θ and ω scan modes. The method of empirical absorption correction was adopted. SHELXTL-97 software was used to solve the structures of **1**–**12** and refine the data.[1] In **1**−**12**, most non-H atoms are refined anisotropically, and only some of water molecules were excepted. H atoms linked to the C and N atoms were were fixed in their ideal positions. To get reasonable thermal parameters and atom sites, some commands such as “isor”

and “dfix” were utilized. Table S4 S5 summarizes the structural determination and crystallographic data for **1**–**12**.

The CCDC reference numbers for compounds **1**–**12** are 1871471−1871482, respectively.

II. Supplementary structure figures

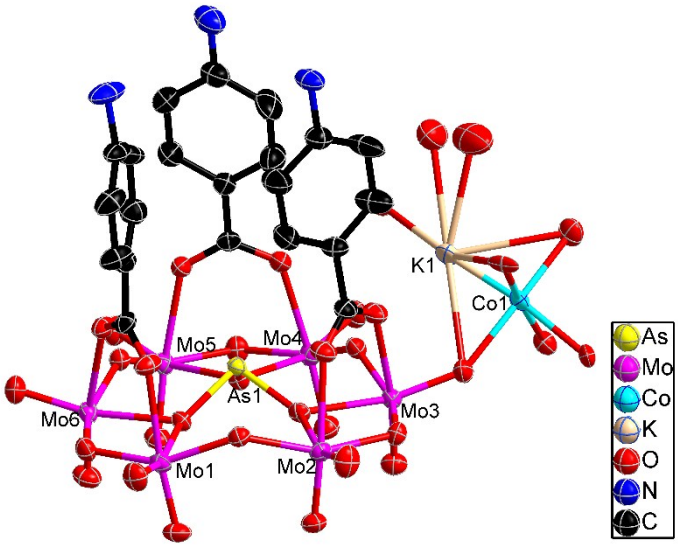

Fig. S1 ORTEP drawing of **1** with thermal ellipsoids at 50% probability. Free water molecules are omitted for clarity. (color code: Co light blue, Mo purple, As yellow, K Tan, O red, N blue, C black).

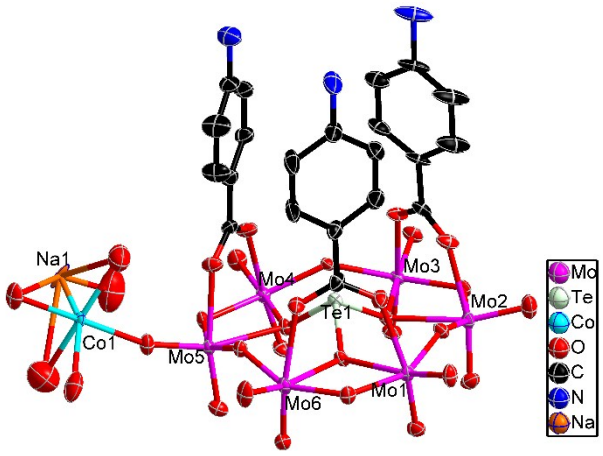

Fig. S2 ORTEP drawing of **5** with thermal ellipsoids at 50% probability. Free water molecules are omitted for clarity. (color code: Co light blue, Na, orange, Mo purple, Te light green, O red, N blue, C black).

Fig. S3 View of the 1D supramolecular chain for **1**.

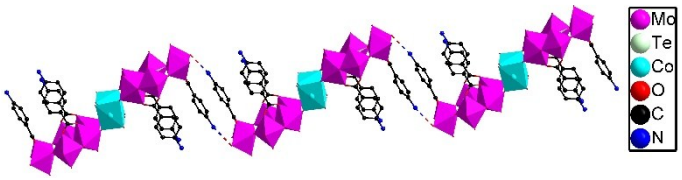

Fig. S4 View of the 1D supramolecular chain for **5**.

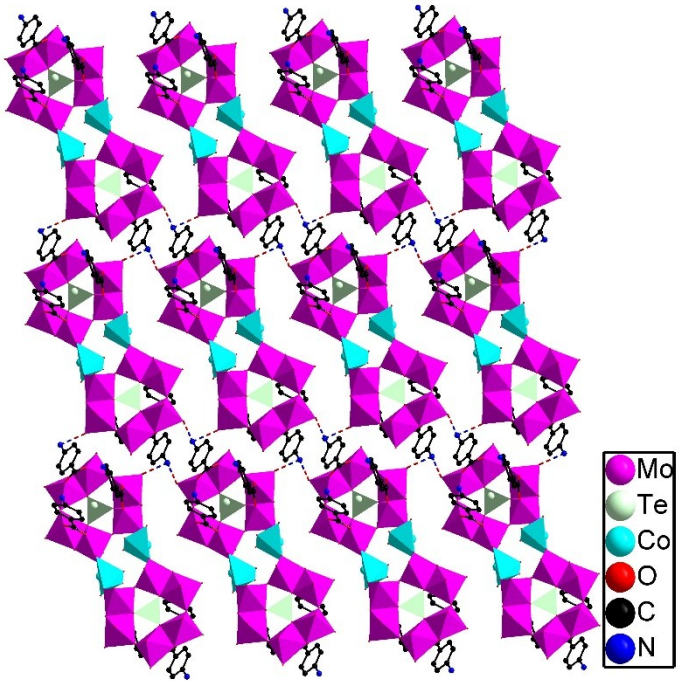

Fig. S5 View of the 2D supramolecular framework showing the hydrogen bonds in **5**.

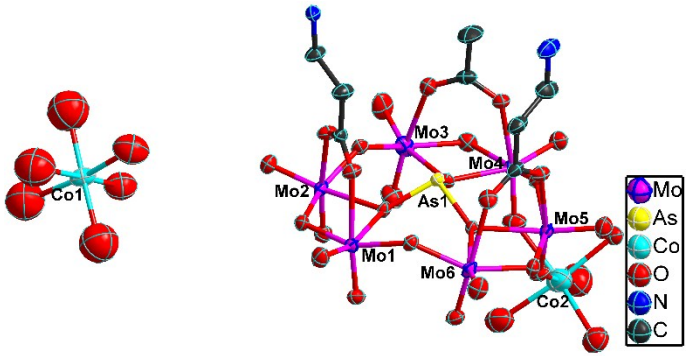

Fig. S6 ORTEP drawing of **9** with thermal ellipsoids at 50% probability. Free water molecules are omitted for clarity. (color code: Co light blue, Mo purple, As yellow, O red, N blue, C black).

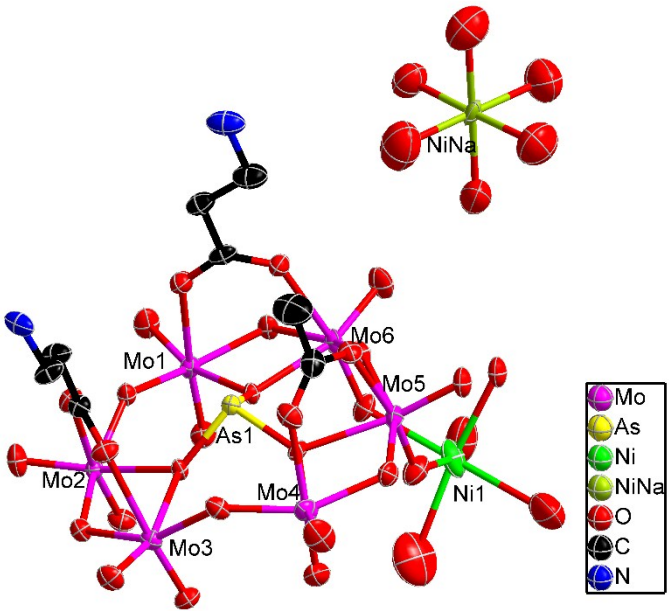

Fig. S7 ORTEP drawing of **10** with thermal ellipsoids at 50% probability. Free water molecules are omitted for clarity. (color code: Ni Bright green, NiNa Lime, Mo purple, As yellow, O red, blue, C black).

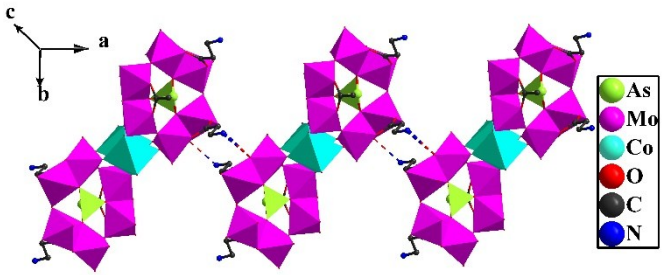

Fig. S8 View of the 1D supramolecular chain in **9**.

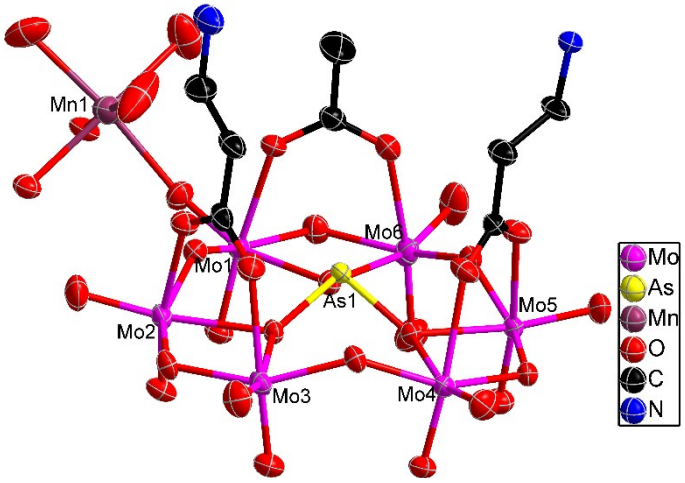

Fig. S9 ORTEP drawing of **12** with thermal ellipsoids at 50% probability. Free water molecules are omitted for clarity. (color code: Mo purple, Mn plum, As yellow, O red, N blue, C black).

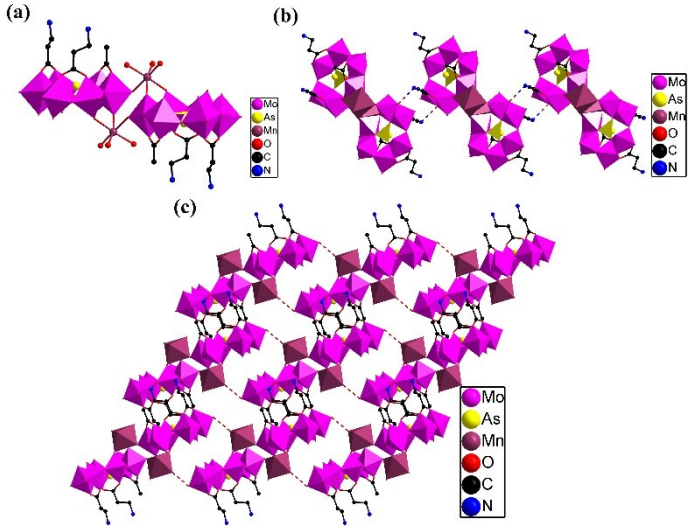

Fig. S10 a) Ball-stick and polyhedral representation of dimeric polyanion for **12;** b) View of the 1D supramolecular chain; c) View of the 2D supramolecular framework showing the hydrogen bonds.

III. Supplementary physical characterizations

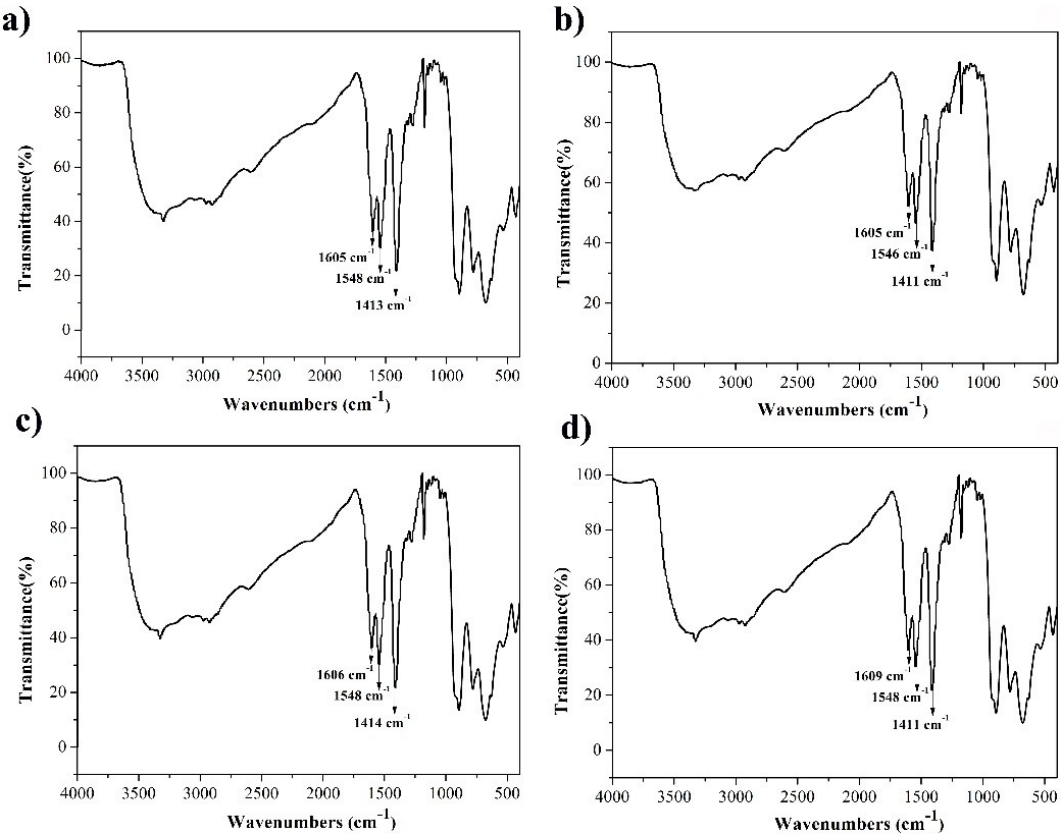

Fig. S11 a b c d) IR spectra for compounds **1**–**4.** The peaks from 400 to 1000 cm^{-1} are similar for the four compounds, which ascribe to the same skeletal vibrations of $\{AsMo_6O_{21}\}$ anions. The characteristic vibrational bands of the organic ligands are located in the region between 1100 and 1650 cm^{-1}. While the absorption maxima at 1607, 1548, and 1413 cm^{-1} for **1** are indicative of the ν_{as}(COO) and ν_s(COO) stretching frequencies, which demonstrates the bidentate coordination mode of the carboxylate group in **1**−**4**.

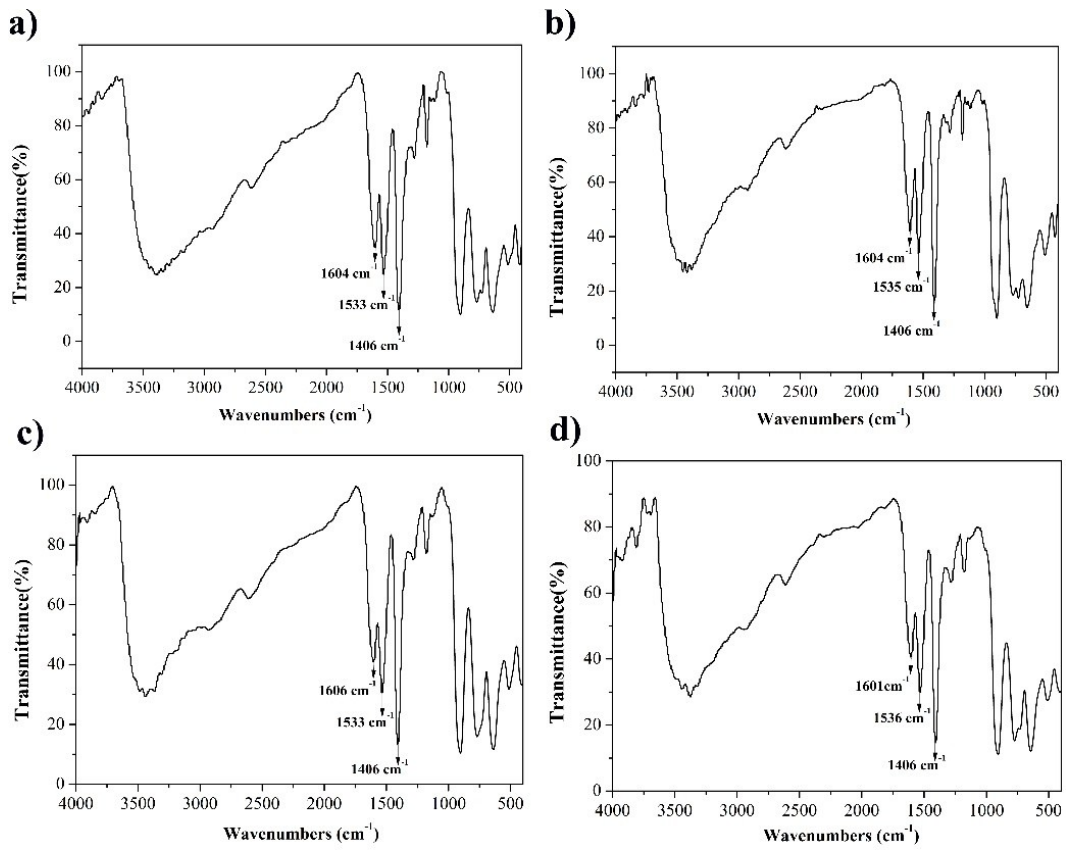

Fig. S12 a b c d) IR spectra for compounds **5–8.** The peaks from 400 to 1000 cm^{-1} are similar for the four compounds, which ascribe to the same skeletal vibrations of $\{TeMo_6O_{21}\}$ anions. The characteristic vibrational bands of the organic ligands are located in the region between 1100 and 1650 cm^{-1}. While the absorption maxima at 1604, 1533, and 1406 cm^{-1} for **5** are indicative of the ν_{as}(COO) and ν_s(COO) stretching frequencies, which demonstrates the bidentate coordination mode of the carboxylate group in **5**−**8**.

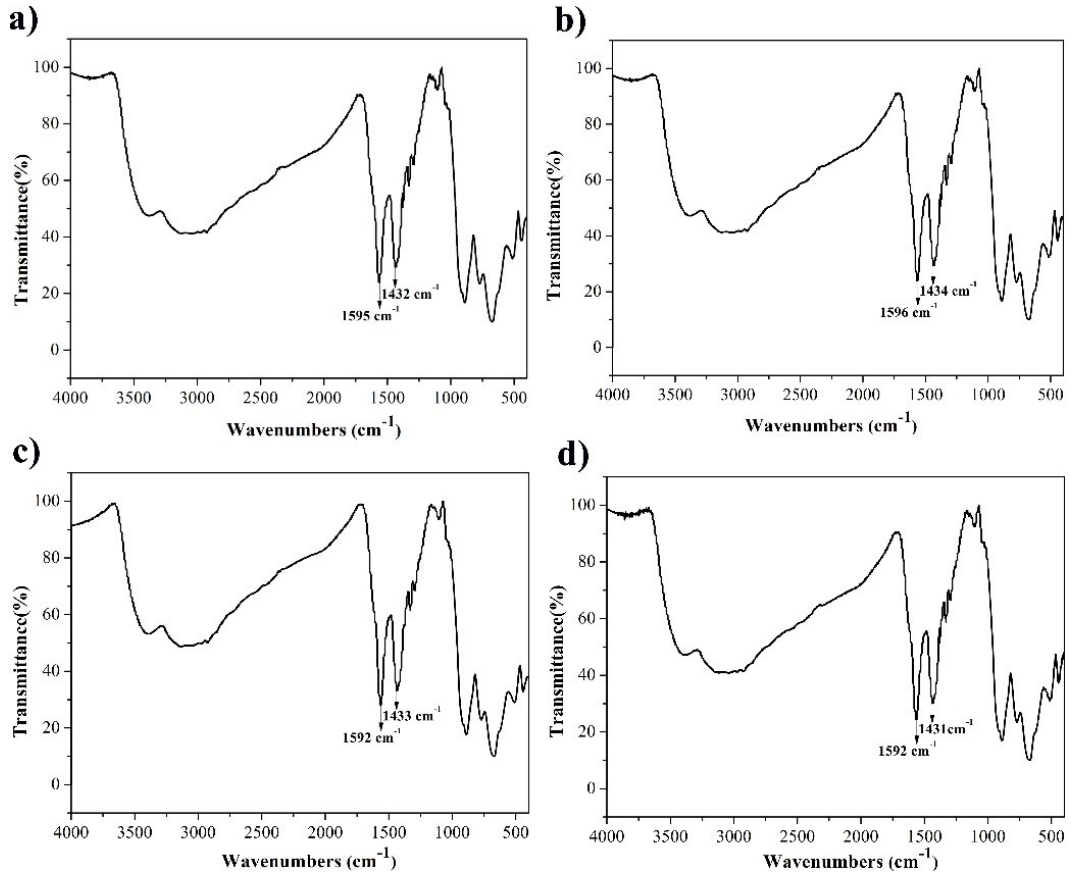

Fig. S13 a b c d) IR spectra for compounds **9–12.** The peaks from 400 to 1000 cm^{-1} are similar for the four compounds, which ascribe to the same skeletal vibrations of $\{AsMo_6O_{21}\}$ anions. The characteristic vibrational bands of the organic ligands are located in the region between 1100 and 1650 cm^{-1}. While the absorption maxima at 1595, and 1432 cm^{-1} for **9** are indicative of the ν_{as}(COO) and ν_s(COO) stretching frequencies, which demonstrates the bidentate coordination mode of the carboxylate group in **9−12**.

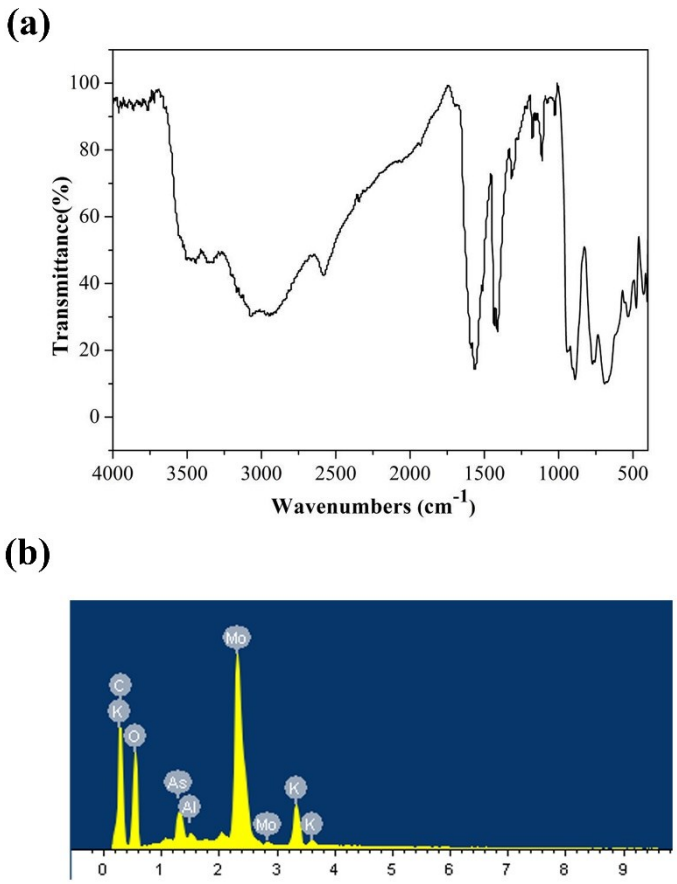

Fig. S14 a) IR spectrum for compound **13**; b) EDS for compound **13**.

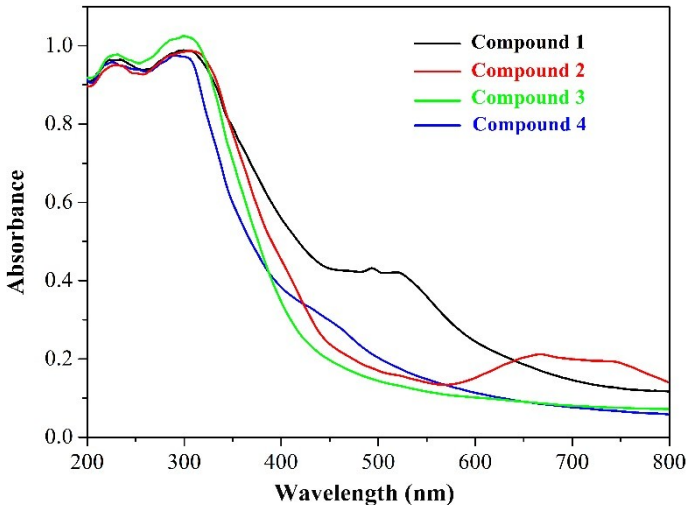

Fig. S15 UV−vis diffuse reflectance spectra of compounds **1**–**4**. The diffuse reflectance spectra of twelve solid samples were detected to obtain the absorption bands located in both the ultraviolet and visible regions. Two intense absorption peaks located in 230 and 300 nm for **1**, 229 and 301 nm for **2**, 228 and 303 nm for **3**, and 225 and 296 nm

for **4** in the UV region, which are assigned to O → Mo charge transfer for $\{AsMo_6O_{21}\}$ polyoxoanions. In the visible region (400–800 nm), the plots display absorption bands at 493 nm and 525 nm for **1**, 668 nm and 745 nm for **2**, 450 nm for **4**, which were respectively assigned to the $^4T_{1g} \rightarrow {}^4T_{2g}$ and $^4A_{2g} \rightarrow {}^4T_{1g}$ for low-spin Co^{2+}, $^3A_{1g} \rightarrow {}^3T_{2g}$ and $^3A_{2g} \rightarrow {}^3T_{1g}$ for Ni^{2+}, and $^4T_{1g} \rightarrow {}^6A_{1g}$ for Mn^{2+}.

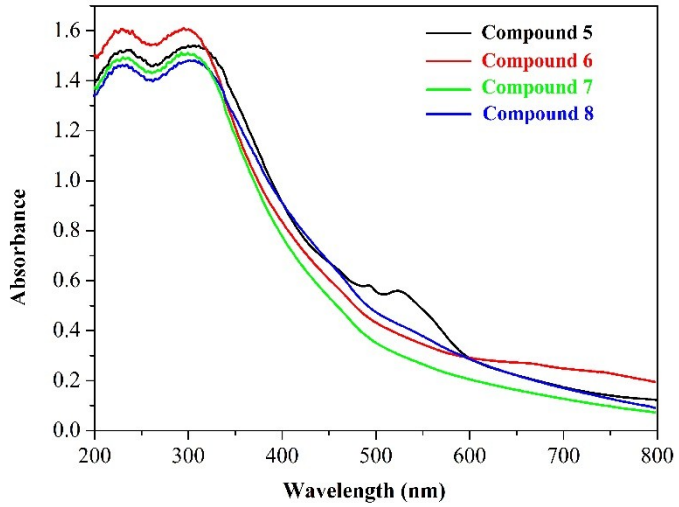

Fig. S16 UV−vis diffuse reflectance spectra of compounds **5**–**8**.

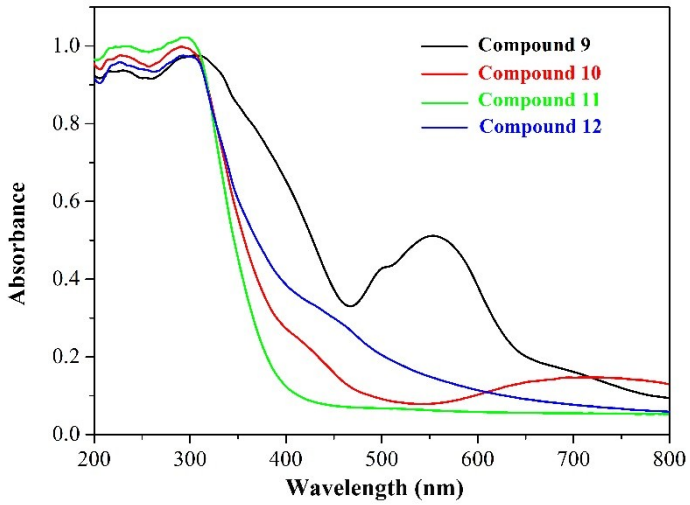

Fig. S17 UV−vis diffuse reflectance spectra of compounds **9**–**12**.

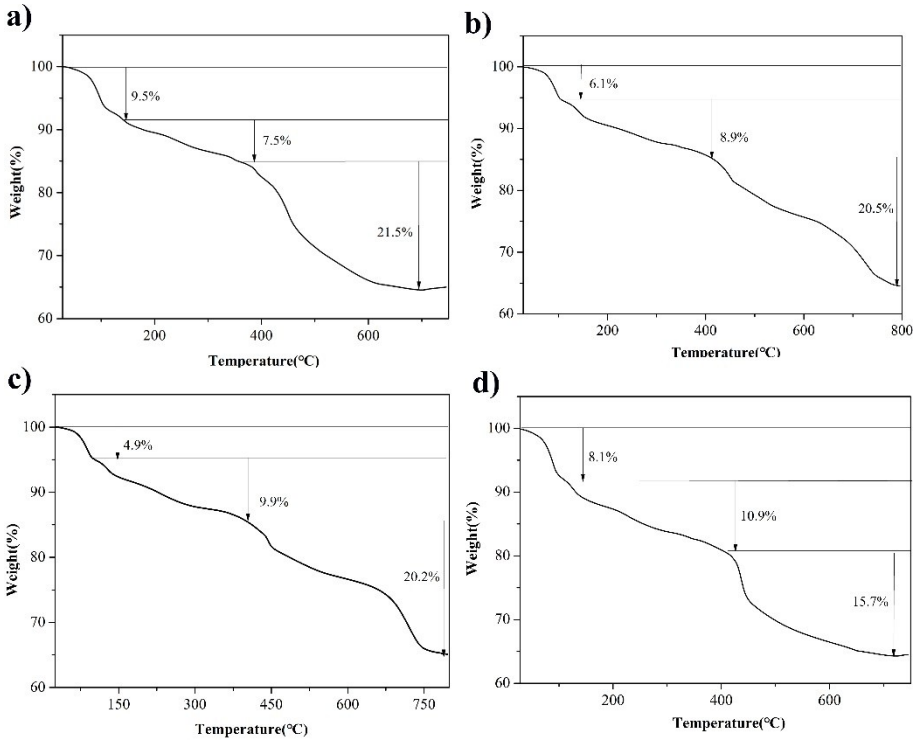

Fig. S18 a b c d) Thermogravimetric plots of compounds **1**–**4**.

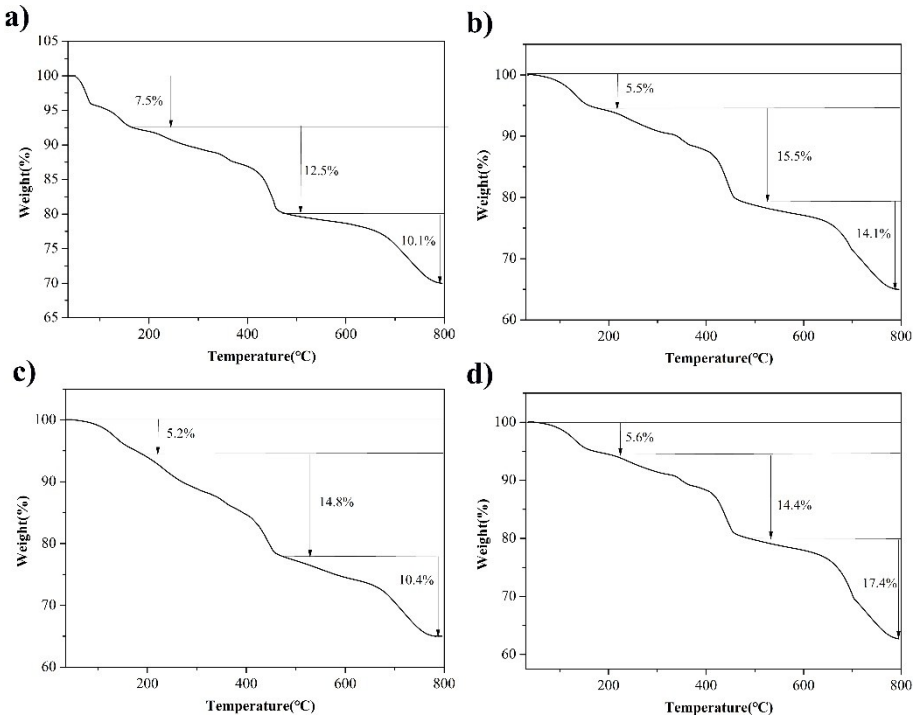

Fig. S19 a b c d) Thermogravimetric plots of compounds **5**–**8**.

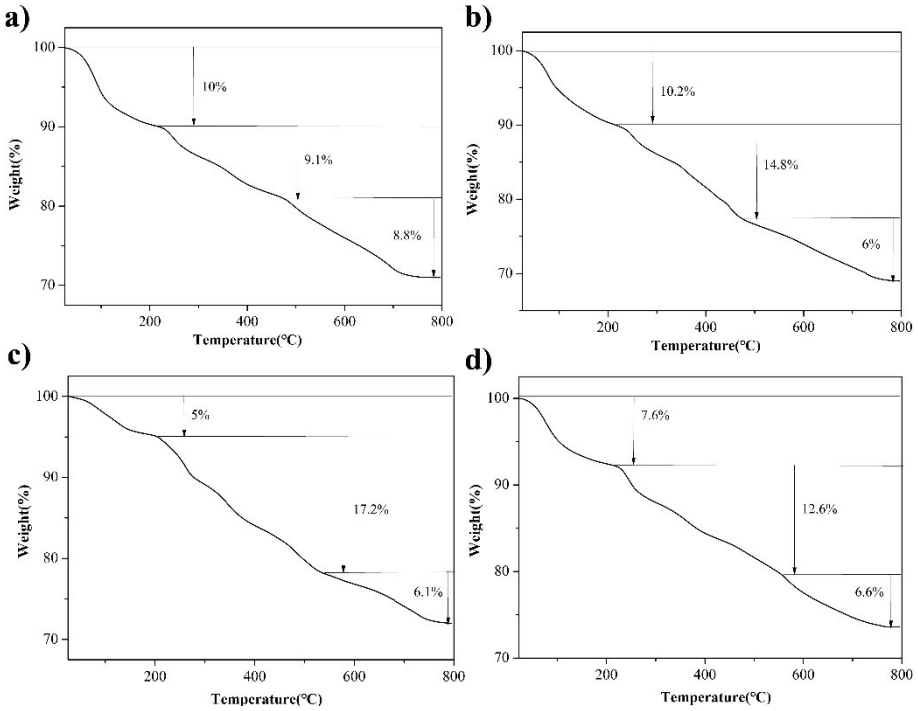

Fig. S20 a b c d) Thermogravimetric plots of compounds **9**–**12**.

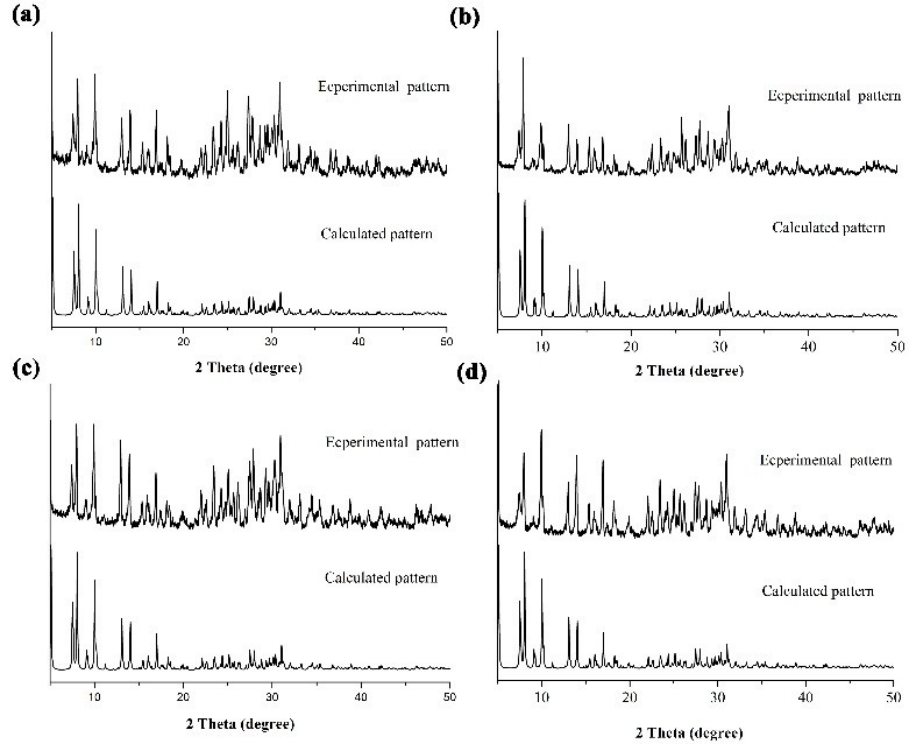

Fig. S21 a b c d) The calculated and experimental PXRD patterns for compounds **1**–**4**.

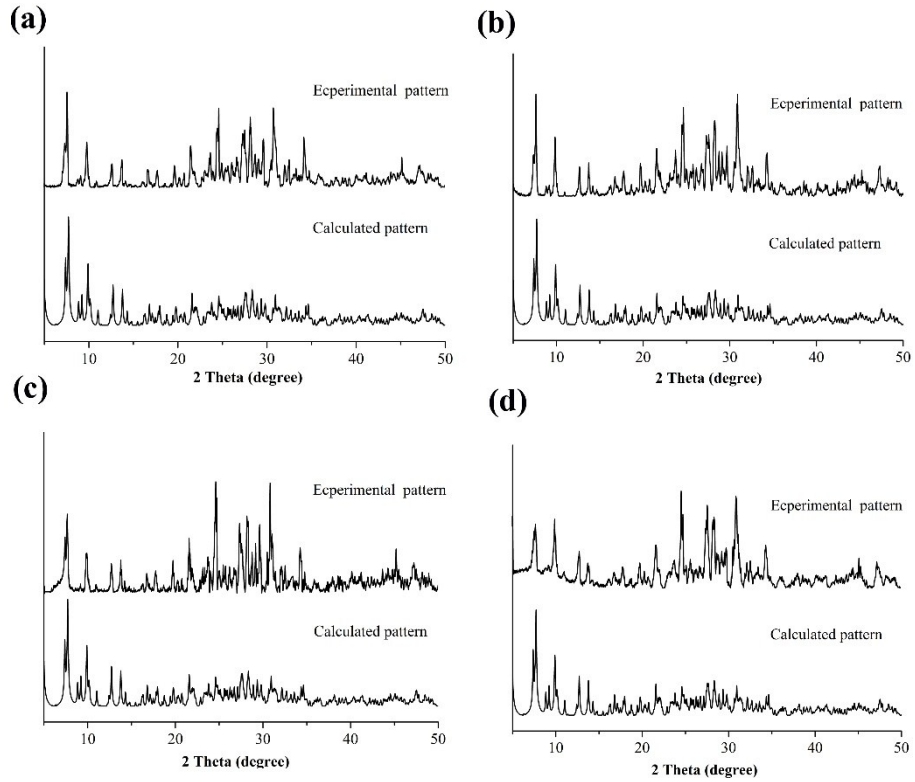

Fig. S22 a b c d) The calculated and experimental PXRD patterns for compounds **5**–**8**.

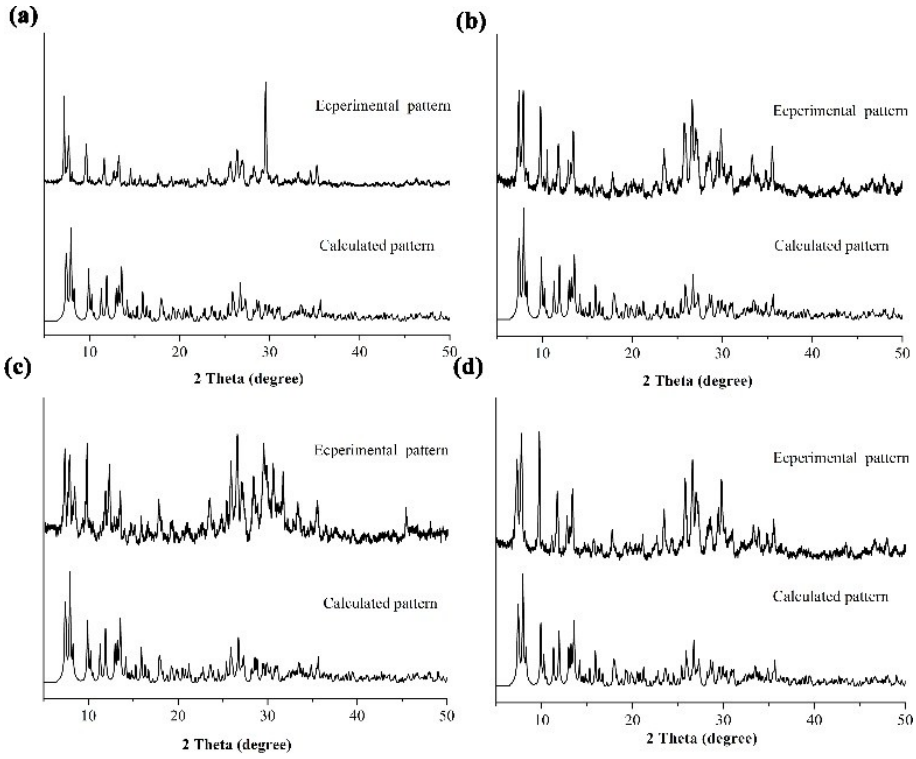

Fig. S23 a b c d) The calculated and experimental PXRD patterns for compounds **9**–**12**.

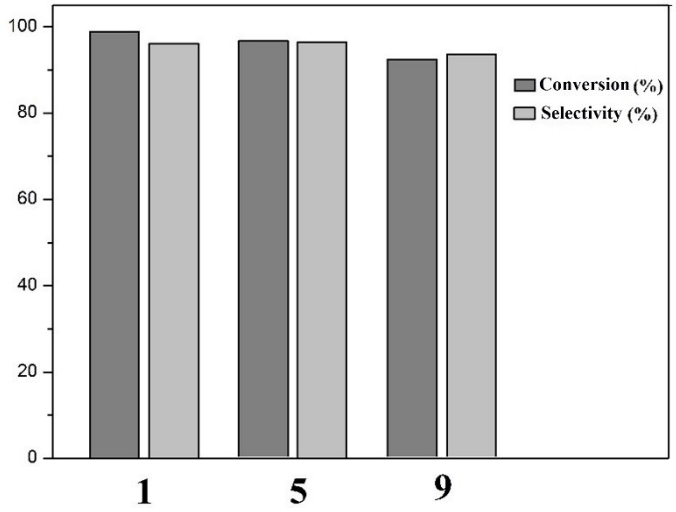

Fig. S24 The comparison of conversion and selectivity of CEES oxidation for compounds **1**, **5** and **9** under similar conditions.

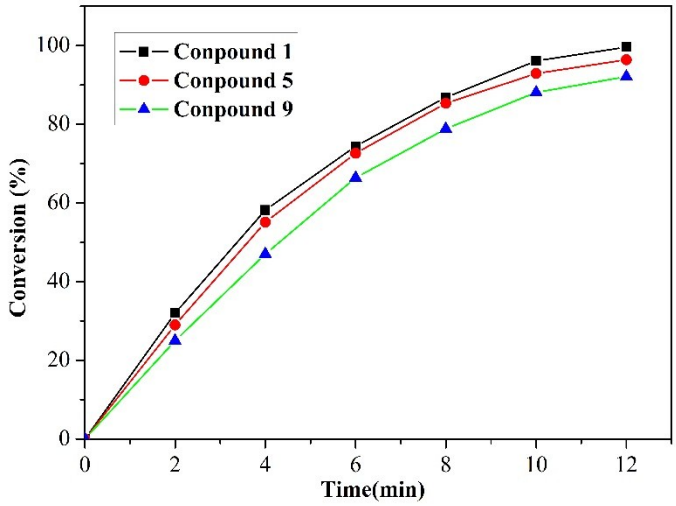

Fig. S25 Time profile for the oxidative decontamination of CEES using **1**, **5**, and **9** with the similar conditions.

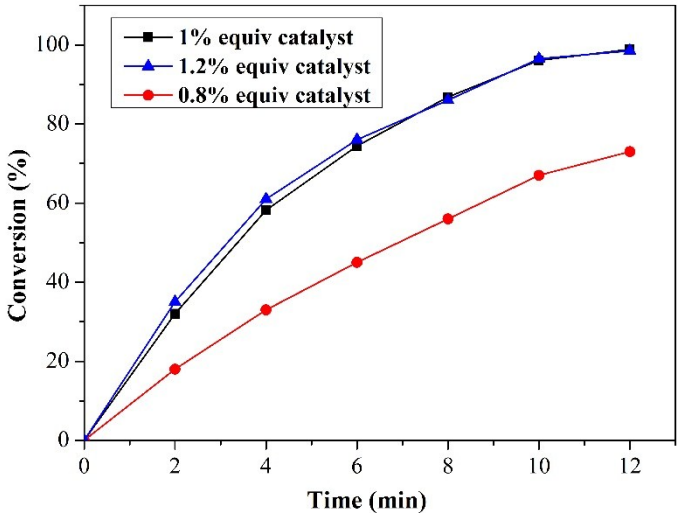

Fig. S26 Time profile for the oxidative decontamination of CEES using **1** with 1 %, 1.2% and 0.8 % equiv. catalyst.

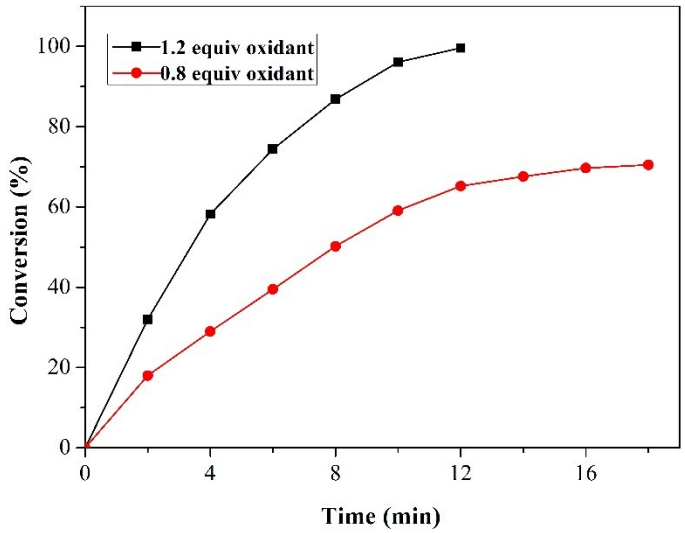

Fig. S27 Time profile for the oxidative decontamination of CEES using **1** with 1.2 and 0.8 equiv. oxidant.

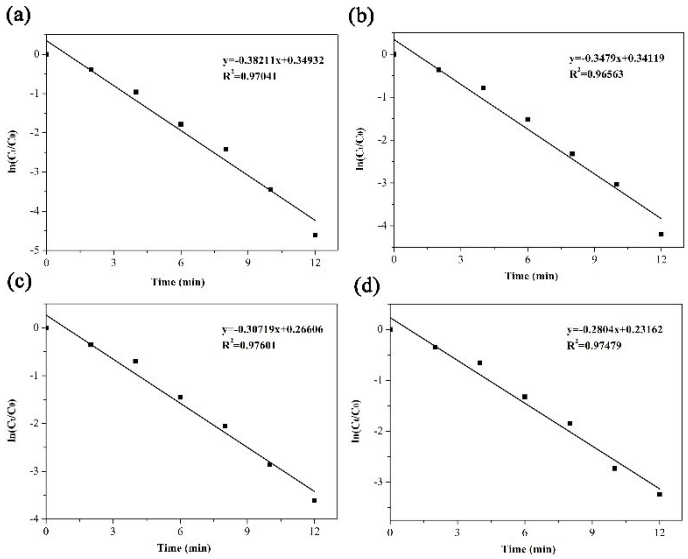

Fig. S28 a b c d) Kinetic analysis of CEES oxidation for compounds **1**–**4** ($\ln(C_t/C_0)$ versus reaction time).

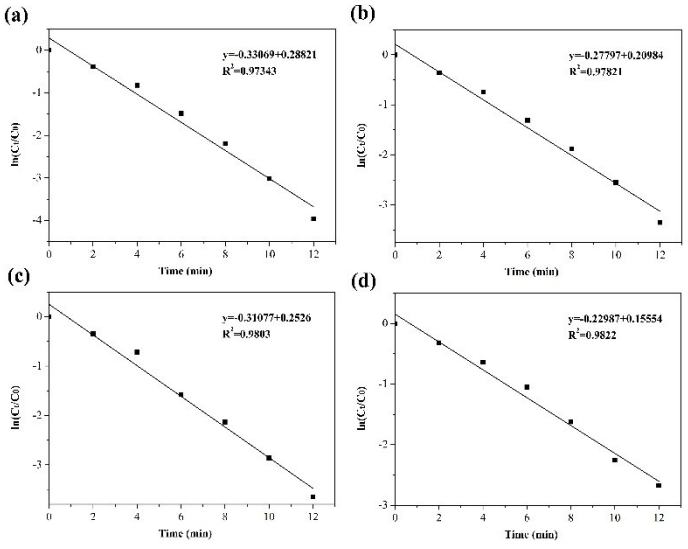

Fig. S29 a b c d) Kinetic analysis of CEES oxidation for compounds **5**–**8** ($\ln(C_t/C_0)$ versus reaction time).

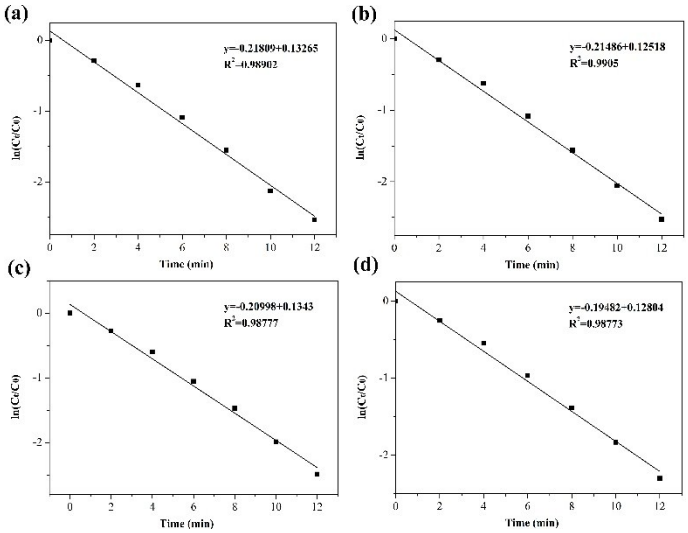

Fig. S30 a b c d) Kinetic analysis of CEES oxidation for compounds **9**–**12** ($\ln(C_t/C_0)$ versus reaction time).

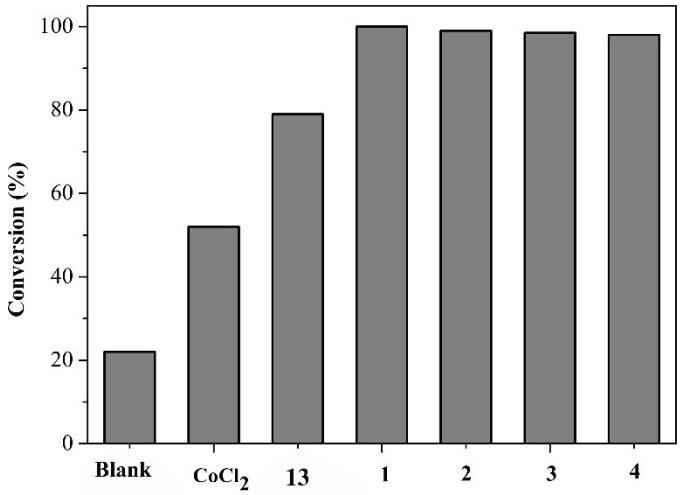

Fig. S31 DECP decomposition by different catalysts. Reaction conditions: [DECP] =1 mmol, 0.6 μmol catalyst, 0.25 mmol naphthalene (internal standard), 600 μL DMF and 50 μL H_2O at room temperature for 10 min.

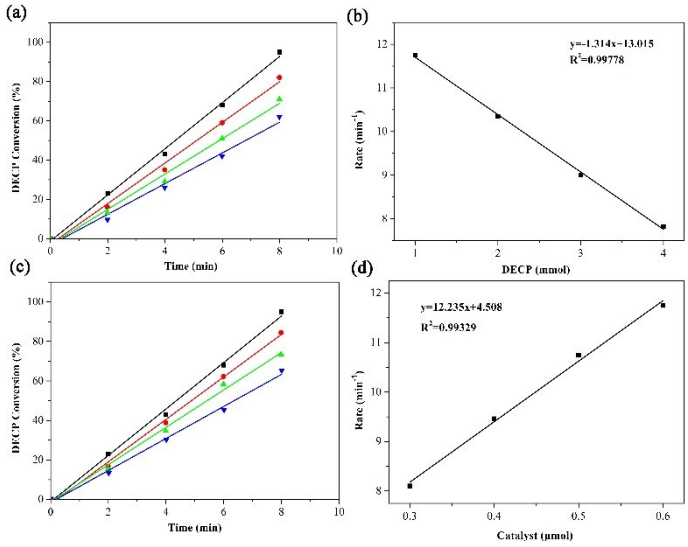

Fig. S32 Kinetic analysis of DECP. a) The DECP conversion by **1**. Line A (black): n[DECP] = 1 mmol, y = 11.75x -1.2, R^2 = 0.99608; Line B (red): n[DECP] = 2 mmol, y = 10.35x - 3, R^2 = 0.99125; Line C (green): n[DECP] = 3 mmol, y = 9x - 3.2, R^2 = 0.98664; Line D (blue): n[DECP] = 4 mmol, y = 7.82x - 3.36, R^2 = 0.98255; b) Plot of the initial rate versus DECP concentration in the decontamination of DECP using **1**; c) Line A (black): the mass of **1**: 1μmol, y =11.75x - 1.2, R^2 = 0.99608; Line B (red): the mass of **1**: 0.75μmol, y = 10.745x - 2.32, R^2 = 0.99604; Line C (green): the mass of **1**: 0.5μmol, y = 9.46x - 1.76, R^2 = 0.99237; Line D (blue): the mass of **1**: 0.25μmol, y = 8.1x - 1.8, R^2 = 0.99353; d) Plot of the initial rate versus the amount of **1** in the decontamination of DECP.

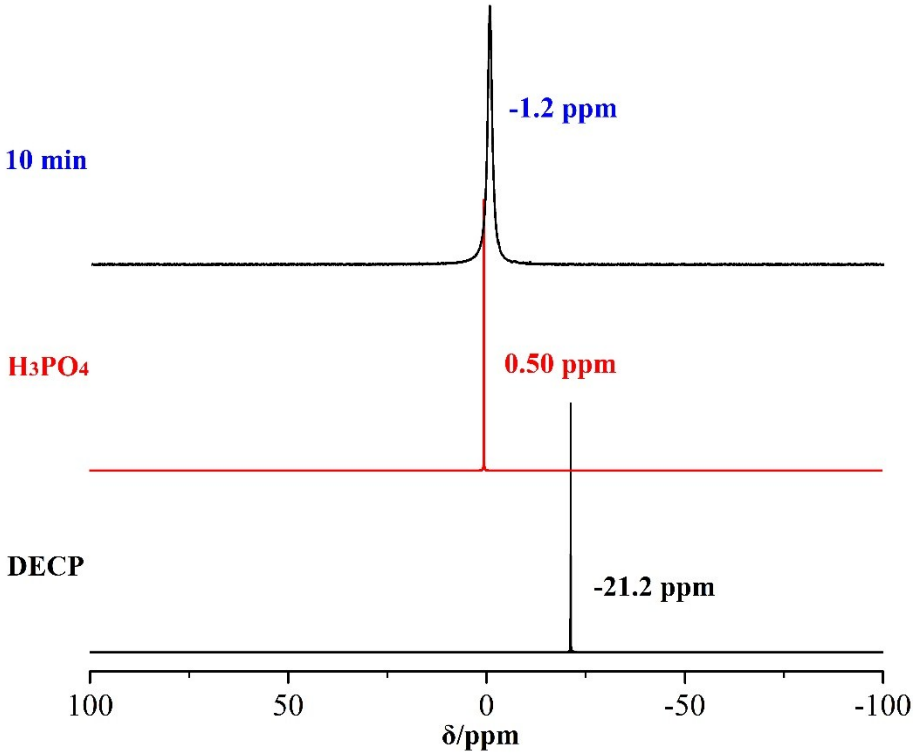

Fig. S33 The ^{31}P NMR spectra of pure DECP (black), phosphates (red) and the catalytic reaction after 10 min (blue). According to the chemical shift of these ^{31}P NMR spectra, we can conclude that the final product for the hydrolysis of DECP is DEHP.

Ⅳ. Supplementary tables

Table S1. The formulas of compounds **1–12.**

Compound	Formula
1	$K_5H[Co(H_2O)_3][AsMo_6O_{21}(O_2C(C_6H_4)NH_3)_2(O_2C(C_6H_4)NH_2)]_2\cdot 17H_2O$
2	$K_5H[Ni(H_2O)_4]$ $[AsMo_6O_{21}(O_2C(C_6H_4)NH_3)_2(O_2C(C_6H_4)NH_2)]_2\cdot 17H_2O$
3	$K_5H[Zn(H_2O)_3]$ $[AsMo_6O_{21}(O_2C(C_6H_4)NH_3)_2(O_2C(C_6H_4)NH_2)]_2\cdot 17H_2O$
4	$K_5H[Mn(H_2O)_4]$ $[AsMo_6O_{21}(O_2C(C_6H_4)NH_3)_2(O_2C(C_6H_4)NH_2)]_2\cdot 18H_2O$
5	$Cs_4Na_2[Co(H_2O)_3][TeMo_6O_{21}(O_2C(C_6H_4)NH_2)_2(O_2C(C_6H_4)NH_3)]_2\cdot 21H_2O$
6	$Cs_4K_2[Ni(H_2O)_3][TeMo_6O_{21}(O_2C(C_6H_4)NH_2)_2(O_2C(C_6H_4)NH_3)]_2\cdot 13H_2O$
7	$Cs_4KH[Zn(H_2O)_2][TeMo_6O_{21}(O_2C(C_6H_4)NH_2)_2(O_2C(C_6H_4)NH_3)]_2\cdot 16H_2O$
8	$Cs_4KH[Mn(H_2O)_3][TeMo_6O_{21}(O_2C(C_6H_4)NH_2)_2(O_2C(C_6H_4)NH_3)]_2\cdot 19H_2O$
9	$Rb_2H_2[Co(H_2O)_6][Co(H_2O)_3][As^{III}Mo_6O_{21}(O_2CCH_2CH_2NH_3)_2(O_2CCH_3)]_2\cdot 12H_2O$
10	$Rb_2H[Na_{0.5}Ni_{0.5}(H_2O)_6]_2[Ni(H_2O)_2][As^{III}Mo_6O_{21}(O_2CCH_2CH_2NH_3)_2(O_2CCH_3)]_2\cdot 18H_2O$
11	$Rb_2H_2[Zn(H_2O)_6][Zn(H_2O)_3][As^{III}Mo_6O_{21}(O_2CCH_2CH_2NH_3)_2(O_2CCH_3)]_2\cdot 14H_2O$
12	$K_2NaH[Mn(H_2O)_3]_2[As^{III}Mo_6O_{21}(O_2CCH_2CH_2NH_3)_2(O_2CCH_3)]_2\cdot 12H_2O$

Table S2. Oxidation of CEES under different solvents catalyzed by compound **1**.

Entry	Catalyst loading (%)	oxidant	Time (min)	Solvent	Conversion (%)	Selectivity (%)
1	1	H_2O_2	12	Acetonitrile	98.9	98.0
2	1	H_2O_2	12	Ethanol	97.8	98.1
3	1	H_2O_2	12	Methanol	98.6	98.0
4	1	H_2O_2	12	ethyl acetate	64.0	82.4

Table S3. Effects of the amount of compound **1** on CEES degradation.

Catalyst loading (%)	Conversion (%)	TOF (h^{-1})
0.8	73.0	456
1.0	98.9	495
1.2	98.5	410

Table S4 Crystal data and structure refinement for **1**–**12**

Complex	**1**	**2**	**3**	**4**
formula	$C_{42}H_{81}N_6O_{74}Mo_{12}K_5CoAs_2$	$C_{42}H_{83}N_6O_{75}Mo_{12}K_5NiAs_2$	$C_{42}H_{81}N_6O_{74}Mo_{12}K_5ZnAs_2$	$C_{42}H_{85}N_6O_{76}Mo_{12}K_5MnAs_2$
formula weight	3409.68	3427.45	3416.14	3441.72
T (K)	293(2)	293(2)	293(2)	293(2)
crystal system	Triclinic	Triclinic	Triclinic	Triclinic
space group	*P*-1	*P*-1	*P*-1	*P*-1
a (Å)	11.6422(2)	11.6585(5)	11.6516(11)	11.6211(5)
b (Å)	12.1336(2)	12.1103(5)	12.1230(12)	12.0930(5)
c (Å)	17.7687(3)	17.7420(7)	17.7391(17)	17.7264(7)
α (˚)	76.6610(10)	76.859(2)	76.692(2)	76.5010(10)
β (˚)	89.6320(10)	89.702(3)	89.874(2)	89.8460(10)
γ (˚)	84.5510(10)	84.663(3)	84.635(2)	84.7250(10)
U (Å^3)	2430.98(7)	2428.46(17)	2427.2(4)	2411.63(17)
Z	1	1	1	1
μ (mm^{-1})	2.354	2.322	2.304	2.648
reflections collected	8509	11143	8492	8369
independent reflections	6877	8568	6228	7421
R(int)	0.0280	0.0387	0.0343	0.0201
GOF on F^2	1.044	1.025	1.057	0.0958
R_1[a] [I> 2σ(I)]	0.0372	0.0413	0.0471	0.0288
wR_2[b] [I> 2σ(I)]	0.0919	0.1061	0.1148	0.0736
R_1 (all data)	0.0495	0.0583	0.0699	0.0336
wR_2 (all data)	0.1007	0.1149	0.1309	0.0765

Complex	**5**	**6**	**7**	**8**
formula	$C_{42}H_{86}N_6O_{78}Mo_{12}Cs_4CoNa_2Te_2$	$C_{42}H_{70}N_6O_{70}Mo_{12}Cs_4NiK_2Te_2$	$C_{42}H_{75}N_6O_{72}Mo_{12}Cs_4ZnKTe_2$	$C_{42}H_{83}N_6O_{76}Mo_{12}Cs_4MnKTe_2$
formula weight	3966.20	3854.07	3858.69	3920.30
T (K)	220(2)	220(2)	220(2)	220(2)
crystal system	Triclinic	Triclinic	Triclinic	Triclinic
space group	*P*-1	*P*-1	*P*-1	*P*-1
a (Å)	11.7267(12)	11.686(9)	11.6855(4)	11.651(3)
b (Å)	12.4654(13)	12.336(10)	12.3860(6)	12.303(4)
c (Å)	18.6945(19)	18.569(15)	18.6191(8)	18.630(5)
α (˚)	74.384(4)	75.760(14)	74.699(3)	74.094(12)
β (˚)	85.990(4)	86.017(13)	85.651(3)	85.386(13)
γ (˚)	84.238(4)	84.106(12)	83.954(3)	84.132(12)
U (Å^3)	2615.9(5)	2578(4)	2581.64(19)	2551.0(13)
Z	1	1	1	1
μ (mm^{-1})	2.518	2.482	2.482	2.552
reflections collected	9176	8220	8686	8217
independent reflections	8301	6971	7206	7259
R(int)	0.0325	0.0463	0.0476	0.0556
GOF on F^2	1.021	1.030	1.046	1.048
R_1[a] [I> 2σ(I)]	0.0375	0.0594	0.0508	0.0504
wR_2[b] [I> 2σ(I)]	0.0956	0.1661	0.1340	0.1403
R_1 (all data)	0.0418	0.0687	0.0619	0.0556
wR_2 (all data)	0.0982	0.1758	0.1420	0.1452

Complex	**9**	**10**	**11**	**12**
formula	$C_{16}H_{78}N_4O_{75}Mo_{12}Rb_2Co_2As_2$	$C_{16}H_{99}N_4O_{86}Mo_{12}Rb_2Ni_2NaAs_2$	$C_{16}H_{82}N_4O_{77}Mo_{12}Rb_2Zn_2As_2$	$C_{16}H_{71}N_4O_{72}Mo_{12}K_2Mn_2NaAs_2$
formula weight	3116.74	3336.46	3165.70	2983.96
T (K)	293(2)	293(2)	293(2)	293(2)
crystal system	Monoclinic	Monoclinic	Monoclinic	Monoclinic
space group	*P*21/c	*P*21/c	*P*21/c	*P*21/c
a (Å)	13.8787(3)	13.8420(4)	13.8717(9)	13.702(2)
b (Å)	23.7424(5)	23.8125(8)	23.7484(13)	23.542(3)
c (Å)	15.8044(3)	14.9785(6)	15.8204(9)	15.546(2)
α (˚)	90.00	90.00	90.00	90.00
β (˚)	120.0320(10)	113.996(2)	119.884(4)	119.466(11)
γ (˚)	90.00	90.00	90.00	90.00
U (Å^3)	4508.60(16)	4510.4(3)	4518.8(5)	4366.0(10)
Z	2	2	2	2
μ (mm^{-1})	2.362	2.321	2.287	2.308
reflections collected	7949	7942	7942	7675
independent reflections	6957	6246	6803	6761
R(int)	0.0326	0.0430	0.0312	0.0394
GOF on F^2	1.137	1.056	1.189	1.047
R_1[a] [I> 2σ(I)]	0.0556	0.0481	0.0753	0.0474
wR_2[b] [I> 2σ(I)]	0.1483	0.0979	0.1729	0.1329
R_1 (all data)	0.0644	0.0678	0.0871	0.0579
wR_2 (all data)	0.1483	0.1056	0.1779	0.1412

[a] $R1 = \sum||F_0|-|F_C||/\sum|F_0|$; [b] $wR2 = \sum[w(F_0^2-F_C^2)^2]/\sum[w(F_0^2)^2]^{1/}$

Table S5. Selected bond lengths (Å) and angles (°) for **1**–**12**.

Compound **1**			
Mo(1)-O(11)	1.712(4)	Mo(2)-O(1)	2.164(4)
Mo(3)-O(17)	1.710(4)	Mo(4)-O(19)	2.282(4)
Mo(5)-O(23)	1.710(4)	Mo(6)-O(25)	2.337(4)
K(1)-O(16)	2.753(5)	K(3)-O(3)	3.033(4)
Co(1)-O(14)	2.000(5)	Co(1)-O(16)	2.046(4)
O(1)-As(1)-O(2)	95.78(18)	O(1)-As(1)-O(3)	96.67(18)
Compound **2**			
Mo(1)-O(8)	1.710(4)	Mo(2)-O(23)	2.283(4)
Mo(3)-O(14)	2.205(4)	Mo(4)-O(5)	1.710(4)
Mo(5)-O(10)	1.714(4)	Mo(6)-O(14)	2.185(4)
K(1)-O(10)	2.811(6)	K(2)-O(13)	2.707(5)
Ni(1)-O(6)	1.972(5)	Ni(1)-O(17)	2.010(4)
O(26)-As(1)-O(14)	95.87(16)	O(26)-As(1)-O(4)	96.70(15)
Compound **3**			
Mo(1)-O(2)	1.722(6)	Mo(2)-O(4)	1.693(6)
Mo(3)-O(16)	1.891(6)	Mo(4)-O(1)	2.322(6)
Mo(5)-O(12)	1.705(6)	Mo(6)-O(13)	2.296(6)
K(1)-O(6)	2.710(4)	K(1)-O(10)	2.786(4)
Zn(1)-O(2)	1.997(6)	Zn(1)-O(15)	2.035(6)
O(17)-As(1)-O(10)	96.2(2)	O(18)-As(1)-O(17)	96.6(2)
Compound **4**			
Mo(1)-O(9)	1.714(3)	Mo(2)-O(1)	1.710(3)
Mo(3)-O(13)	2.298(3)	Mo(4)-O(3)	1.912(3)
Mo(5)-O(15)	2.277(3)	Mo(6)-O(5)	1.712(3)
K(1)-O(1)	2.688(4)	K(1)-O(9)	2.866(4)
Mn(1)-O(22)	2.087(4)	Mn(1)-O(16)	2.027(4)
O(24)-As(1)-O(10)	95.95(13)	O(10)-As(1)-O(27)	96.62(13)

Compound **5**			
Mo(1)-O(5)	1.711(5)	Mo(2)-O(27)	2.284(5)
Mo(3)-O(8)	1.709(5)	Mo(4)-O(26)	2.262(5)
Mo(5)-O(11)	1.714(5)	Mo(6)-O(14)	2.245(4)
Cs(1)-O(8)	3.194(5)	Cs(2)-O(3)	3.056(5)
Co(1)-O(13)	2.110(5)	Co(1)-O(23)	2.133(6)
O(2)-Te(1)-O(7)	94.04(18)	O(14)-Te(1)-O(2)	93.70(18)
Compound **6**			
Mo(1)-O(1)	1.709(9)	Mo(2)-O(10)	2.302(8)
Mo(3)-O(2)	1.746(9)	Mo(4)-O(4)	2.305(7)
Mo(5)-O(13)	1.726(8)	Mo(6)-O(9)	2.279(8)
Cs(2)-O(25)	3.111(8)	Cs(1)-O(22)	3.687(9)
Ni(1)-O(3)	2.043(10)	Ni(1)-O(1)	2.016(11)
O(11)-Te(1)-O(19)	93.4(3)	O(19)-Te(1)-O(18)	94.1(3)
Compound **7**			
Mo(1)-O(14)	1.708(7)	Mo(2)-O(16)	2.282(7)
Mo(3)-O(18)	1.921(6)	Mo(4)-O(1)	1.710(6)
Mo(5)-O(5)	1.916(6)	Mo(6)-O(19)	1.721(7)
Zn(1)-O(21)	2.083(7)	Zn(1)-O(19)	2.112(8)
O(8)-Te(1)-O(10)	94.4(3)	O(23)-Te(1)-O(8)	93.8(3)
Compound **8**			
Mo(1)-O(1)	1.710(6)	Mo(2)-O(2)	2.268(7)
Mo(3)-O(6)	1.714(7)	Mo(4)-O(8)	2.229(6)
Mo(5)-O(7)	1.928(6)	Mo(6)-O(5)	2.244(6)
Cs(2)-O(27)	3.113(6)	Cs(2)-O(18)	3.268(6)
Mn(1)-O(13)	2.134(7)	Mn(1)-O(1)	2.181(7)
O(15)-Te(1)-O(21)	94.3(3)	O(21)-Te(1)-O(8)	94.4(2)

Compound **9**			
Mo(1)-O(11)	1.940(6)	Mo(2)-O(4)	1.718(6)
Mo(3)-O(18)	1.715(7)	Mo(4)-O(5)	1.703(8)
Mo(5)-O(27)	2.303(7)	Mo(6)-O(22)	1.706(8)
Co(1)-O(18)	2.103(7)	Co(1)-O(10)	2.201(9)
O(13)-As(1)-O(14)	96.3(3)	O(13)-As(1)-O(9)	96.6(3)
Compound **10**			
Mo(1)-O(6)	1.713(6)	Mo(2)-O(23)	1.720(6)
Mo(3)-O(9)	2.325(5)	Mo(4)-O(3)	1.711(5)
Mo(5)-O(13)	2.288(8)	Mo(6)-O(21)	1.706(7)
Ni(1)-O(17)	2.180(6)	Ni(1)-O(23)	2.268(7)
O(20)-As(1)-O(25)	96.3(3)	O(25)-As(1)-O(24)	96.4(3)
Compound **11**			
Mo(1)-O(3)	2.335(9)	Mo(2)-O(7)	1.709(9)
Mo(3)-O(15)	2.221(8)	Mo(4)-O(27)	1.719(10)
Mo(5)-O(5)	1.707(10)	Mo(6)-O(13)	2.220(9)
Zn(1)-O(4)	2.192(10)	Zn(2)-O(9)	2.230(12)
O(13)-As(1)-O(14)	96.1(4)	O(14)-As(1)-O(15)	96.3(4)
Compound **12**			
Mo(1)-O(10)	1.888(4)	Mo(2)-O(2)	2.177(4)
Mo(3)-O(14)	2.294(4)	Mo(4)-O(21)	1.720(4)
Mo(5)-O(22)	1.703(5)	Mo(6)-O(9)	1.683(5)
Mn(1)-O(21)	2.133(4)	Mn(1)-O(13)	2.173(5)
O(7)-As(1)-O(5)	96.36(19)	O(5)-As(1)-O(2)	96.56(18)

(1) (a) Sheldrick. G. M. *SHELXL 97, Program for Crystal Structure Refinement, University of G ttingen,* Germany, **1997.** (b) Sheldrick. G. M. *SHELXL 97, Program for Crystal Structure Solution, University of G ttingen*, Germany, **1997**.